Solid State Science and Technology, Vol. 21, No 1 & 2 (2013) 31-38
ISSN 0128-7389

SYNTHESIS AND CHARACTERIZATION OF NICKEL MANGANESE OXIDE NANOPARTICLES BY THERMAL TREATMENT METHOD

N. Ahad*, A. H. Shaari, E. B. Saion, M. Hashim, J. Hassan, S. A. Bakar

Department of Physics, Faculty of Science, University Putra Malaysia, 43400 Serdang, Malaysia

**Corresponding author: noorhanim_ahad@yahoo.com*

ABSTRACT

Zero dimensional nanomaterials such as nanoparticles, quantum dots and metal oxide nanocrystals of less than 100 nm in dimension are attracted considerable attention in recent years because of their excellent physical and chemical properties that are different from their respective bulk counterparts. In particular spinel metal manganese oxides or manganites nanoparticles are important class of mixed-metal manganese oxides, owing to their diverse properties such as photocatalytic and electrochemical properties. In this research, nickel manganese oxide ($NiMn_2O_4$) nanocrystals were synthesized by a thermal treatment method. The method followed by calcination at various temperatures from 450 to 950°C. In this investigation, we used polyvinyl pyrrolidon (PVP) as a capping agent to control the agglomeration of the nanoparticles. The characterization studies were conducted by X-ray diffraction (XRD) to generate diffraction patterns of crystalline samples at room temperature. The Fourier transform infrared spectroscopy was used to confirm the presence of metal oxide bands at all temperatures and the absence of organic bands at 950 °C. The magnetic properties were measured using an electron spin resonance (ESR).

Keywords: nanoparticles; manganese oxides; thermal treatment;

INTRODUCTION

Recently, many studies have focused on the synthesis of nanomaterials, such as metal oxide nanocrystals, which are attracting significant interest due to their extensive applications. Metal manganese oxide nanocrystals are regarded as the most important nanomaterials because of their magnetic, electrical, optical, electronic and catalytic properties. Spinel manganese oxide have structure AB_2O_4 in which A and B display tetrahedral and octahedral cation sites respectively, and O indicates the oxygen anion site. As one of the important metal oxides with spinel structure, $NiMn_2O_4$ is a promising functional material and has become the focus of various researches owing to its potential applications. For example, $NiMn_2O_4$ have a high activity with respect to the reactions of ozone decomposition and CO and CH oxidation in the presence of ozone at room temperatures [1]. The physical and chemical properties of nanomaterials would be strongly affected by their particle sizes, morphologies [2] and shape [3] which can be controlled in the fabrication processes. Considerable interest in diverse methods for the

synthesis of spinel metal manganese oxide nanoparticles with controllable size, shape, stability, and free from contamination has been devoted for achieving better metal manganese oxides that have the desired physical and chemical properties for a variety of applications. Various fabrication techniques have been reported including chemical, sol-gel [4], co-precipitation [5], hydrothermal [6], microemulsion [7], microwaves [8], ultrasonic spray pyrolysis [9], reverse micelles [10], aerosol [11], and laser ablation [12]. Most the present preparation technique of metal oxide nanomaterials are difficult to apply on a larger scale because of their complicated procedure, high reaction temperatures, long reaction times, toxic reagents and contaminated with by products, and their potential harm to the environment.

In this research, we will implement a new route of synthesis for metal oxide nanoparticles, first introduced for spinel metal ferrites nanoparticles at Universiti Putra Malaysia (UPM), by a simple thermal treatment method [3], [13-15]. Nickel manganese oxide nanocrystals were prepared from an aqueous solution containing metal nitrates, poly (vinyl pyrrolidon), and deionized water using a low temperature treatment method, followed by calcination processes. This method offer several advantages; fast and harmless feature, controllable particle size and size distribution, no reducing chemical agent or catalyst used, a low cost, a lack of by product effluents and an environmentally friendly operation.

MATERIALS AND METHODS

In thermal treatment method for synthesis of nickel manganese oxide nanoparticles, metal nitrate reagents were used as precursors, polyvinyl pyrrolidone (PVP) as caping agent to control the agglomeration of the particles, and deionized water as solvent. Manganese nitrate, $Mn(NO_3)_2.6H_2O$ and nickel nitrate, $Ni(NO_3)_2.6H_2O$ were purchased from Acros Organics. PVP (MW=29,000) was purchased from Sigma Aldrich. All materials were used without further purification. 0.2 mmol manganese nitrate and 0.1 mmol nickel nitrate (Mn:Ni = 2:1) were added into an aqueous solution containing PVP which was prepared by dissolving 3.5 g of polymer in 100 ml of deionized water at 363 K. The mixture was stirred constantly for 2 h using magnetic stirrer until homogenous solution was obtained. The mixed solution was poured into a glass Petri dish and heated at 353 K in an oven for 24 h to evaporate most of the water. No precipitation of materials was observed before putting into the oven. The dried amorphous material that remained was crushed and ground in a mortar to form powder. The calcinations of the powders were conducted at different calcination temperatures from 450°C to 900°C for 3 h to remove the organic matters and crystallize the nanoparticles.

CHARACTERIZATION

The structure of the $NiMn_2O_4$ nanoparticles was characterized by the X-ray diffraction (XRD) technique using a Shimadzu diffract meter model XRD 6000 employing Cu K_α (0.154 nm) radiation to generate diffraction patterns from powder crystalline samples at ambient temperature in the range of $2q = 10^0 – 80^0$. The Fourier transform infrared

Solid State Science and Technology, Vol. 21, No 1 & 2 (2013) 31-38
ISSN 0128-7389

(FTIR) spectroscopy was used to confirm the presence of metal oxide bands at all temperatures and the absence of organic bands at 900°C. Infrared spectra (280 – 4000 cm^{-1}) were recorded using an FTIR spectrometer (Perkin Elmer model 1650). The magnetic properties were measured using an electron spin resonance (ESR). ESR spectra were recorded on a JEOL JES-FA200 ESR spectrometer (JEOL, Tokyo, Japan) at room temperature for spinel manganese oxide nanoparticles which have unpaired electrons.

RESULTS AND DISCUSSION

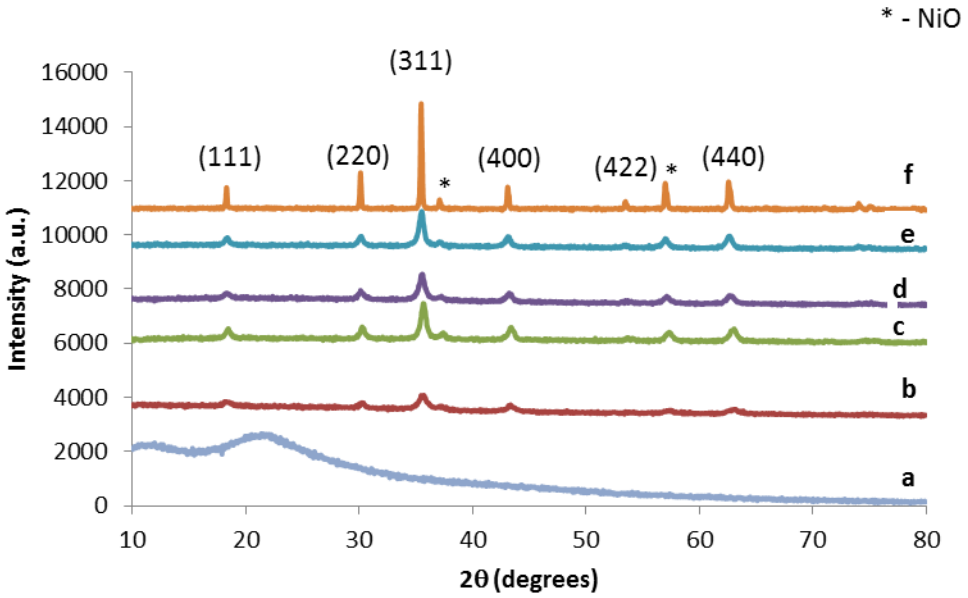

Figure 1: XRD patterns of (a) precursor and nickel manganese oxide nanoparticles calcined at (b) 4500°C, (c) 6500°C, (d) 7500°C, (e) 8500°C and (f) 9500°C

Figure 1 shows the XRD precursor and nickel manganese oxide nanoparticles. A broad peak occurred in the precursor (Figure 1 (a)), which does not have sharp diffraction patterns and still amorphous. The XRD diffraction patterns of nickel manganese oxide nanoparticles at different calcination temperatures of 450, 650, 750,850 and 950°C are shown in Figure 1b, c, d, e and f respectively. The calcined patterns show the reflection planes (111), (220), (311), (400), (422) and (440), which confirm the presence of single-phase $NiMn_2O_4$ with face-centered cubic structure (PDF 00-001-1110) except for phase due to impurity of metal oxides (NiO) were observed in the synthesized sample (Figure 1). Results show that with the increase of the calcination temperature, the diffraction peaks become sharper and increased in intensity. This is due to particle size enlargement of the nuclei which causes the increment of crystalline volume ratio [16].

The average particle size of nickel manganese oxide nanoparticles was determined using Scherer formula:

$$D = 0.9\lambda / \beta \cos\theta$$

Where D is the crystallite size (nm), b is the full width of the diffraction line at half the maximum intensity measured in radians, l is the X-ray wavelength of Cu K_a = 0.154 nm and q is the Bragg angle. The calculated crystallite sizes were found to increase with the calcination temperature, which ranged from 16 ± 1 nm at 450°C to 51 ± 1 nm at 950°C, as shown in Table 1. The results showed that the diffraction peaks became sharper and narrower and increased in intensity when the calcination temperatures increase.

Table 1: Average particle size (nm) of $NiMn_2O_4$ nanoparticles determined from XRD and magnetic properties observed from ESR technique at room temperature for samples calcined at 450, 650,750, 850 and 950°C.

$NiMn_2O_4$ nanoparticles	Calcination temperature (°C)	Average particle size XRD (nm)	Line width DHpp (Oe)	Gromagnetic ratio (g-values)	Magnetic resonance field Hr (Oe)
1	450	16 ± 1	-	-	-
2	650	21 ± 1	-	-	-
3	750	28 ± 1	98.66	2.3202	286.50
4	850	36 ± 1	155.51	2.5453	260.86
5	950	51 ± 1	84.39	2.6166	238.40

The nickel manganese oxide samples were studied further to confirmed the existence of the metal oxide structure using FTIR spectra analysis. Figure 2 shows the FTIR spectra with wave numbers between 280 and 4000 cm^{-1} for precursor and calcined samples. In the previous study by Salker and Gurav, they reported that spinel type oxides exhibit two distinguished bands in wave number range between 400 and 700 cm-^{1} [17]. Figure 2(a) shows all absorption peaks in the precursor attributed to PVP. The peaks are at 3466, 2966, 1660, 1435, 1290, 847 and 581 cm^{-1}, attributed to the stretching and bending vibrations of O-H, C-H, C=O, H-C-H, C-N, C-C and C-N=O, respectively. The vibrational spectra of the absorption bands of pure spinel nickel manganese oxide nanoparticles were observed at 425, 433, 426, 431 and 436 cm^{-1} for the sample calcined at 950, 850, 750, 650 and 450°C respectively. The spectra correspond to the vibration mode of Ni-O-Mn in $NiMn_2O_4$, indicated the formation of the spinel $NiMn_2O_4$ nanostructure as suggested by previously published data [13]. The vibration of ions in the crystal lattice is usually assigned by the infrared (IR) bands of materials. The absence of peaks in the ranges of 1000-1300 cm^{-1} and 2000-3000 cm^{-1} for the sample calcined at 950°C confirmed the non-existence of the O-H mode, C-O mode, and C=H stretching mode of organic sources [18]. This IR analysis is very useful to decisive the temperature of calcination at 950°C by the removing of unwanted ions, which may pollute the crystal lattice during preparation. However, at the lower temperature of 950°C, there were still traces of broadband absorption peaks at 1000-1650 cm^{-1} and 3300-3370 cm^{-1} due to traces of absorbed or atmospheric CO_2 and O-H stretching vibration respectively (Figure 2b-e) [19]. From (Figure 2 (c-f)), the FTIR spectra show the existence bands at 323, 323, 326 and 310 cm-1. These absorption spectra may be

due to Ni-O bond [14]. Figure 2 (b-f) was also showing the spectra at 574, 573, 563,579, and 575 cm-1, correspond to vibration of oxygen atoms in spinel [20].

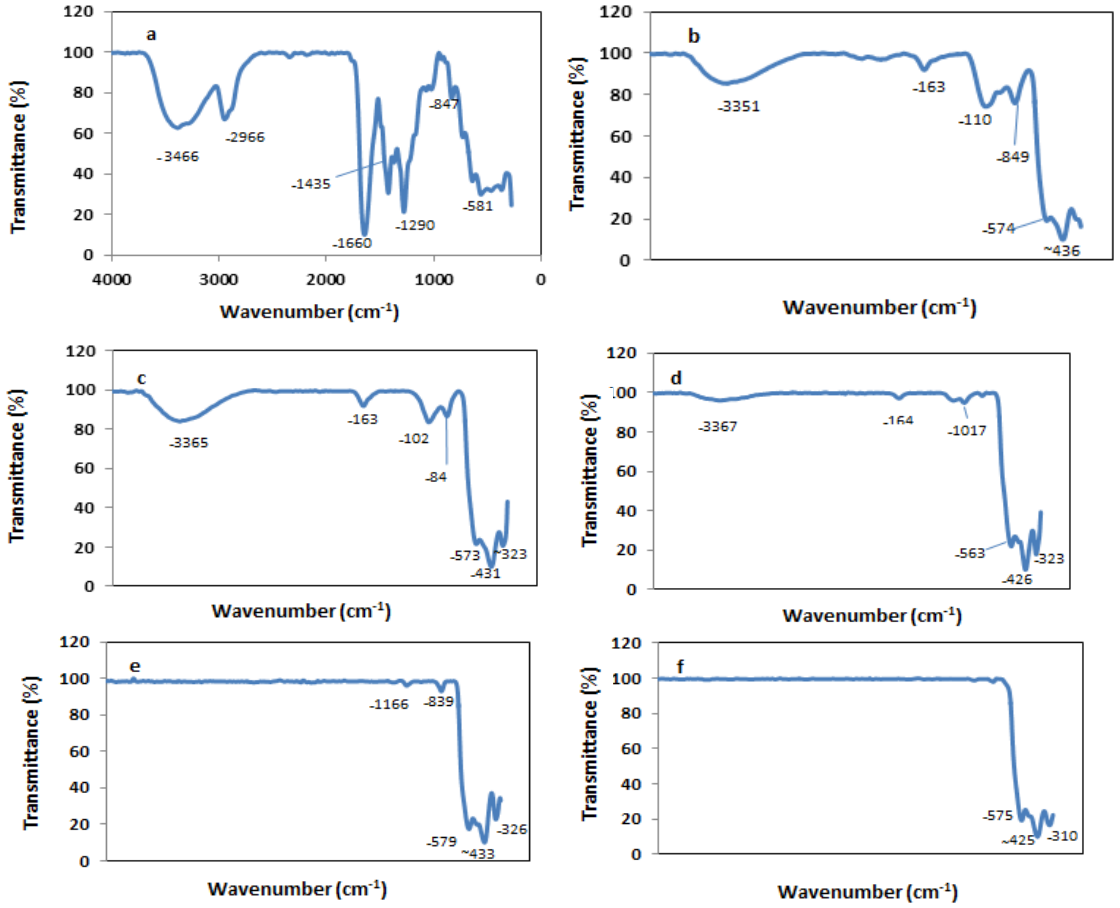

Figure 2: FTIR spectra of (a) precursor and nickel manganese oxide nanoparticles calcined at (b) 450°C, (c) 650°C, (d) 750°C, (e) 850°C and (f) 950°C

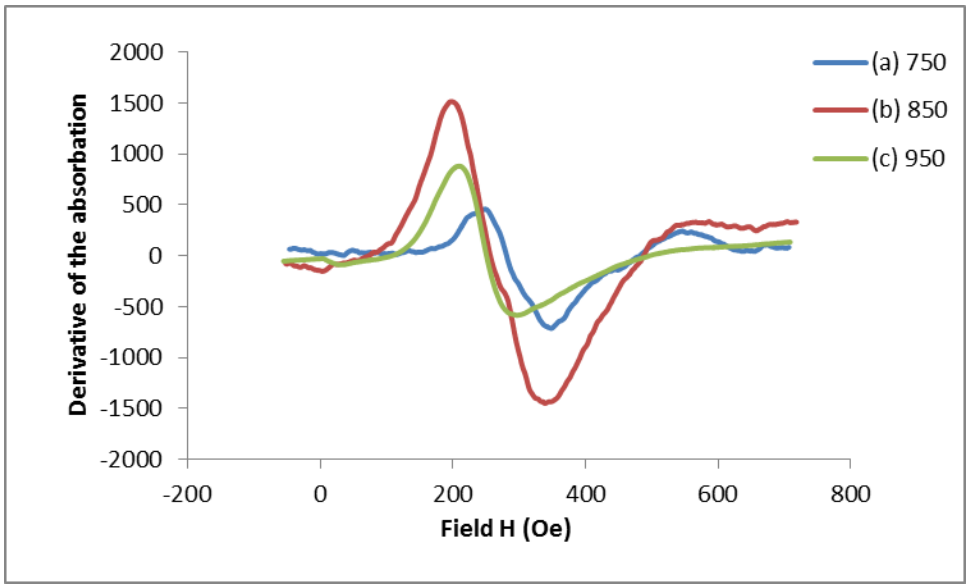

Figure 3: ESR spectra of nickel manganese oxide nanoparticles calcined from 750 to 950°C.

Figure 3 shows the ESR spectra of the nickel manganese oxide nanoparticles calcined at (a) 750, (b) 850 and (c) 950°C. The samples calcined at lower temperature did not exhibit resonance signal relate to ESR spectra. This could be possibly due to the super exchanged interaction produces that occurs in this nanoparticles. Vaidyanathan and Sendhilnathan reported that strong dipole interactions give a large DHpp and g value while strong super exchange interaction produces small value of DHpp and g value [21]. Peak-to-peak line width (DHpp), resonant magnetic field (Hr), and g-factor obtained from ESR measurement are three parameters that characterize the magnetic properties. The values were tabulated in Table 1 and it is obvious that the values of g-factor increase from 2.32 to 2.61 when the calcination temperature and particle size were increased. The result also shows that DHpp values increase from 98.66 to 155.57 and then decrease to 84.39 Oe for samples calcined at 750, 850 and 950°C respectively. The increasing of g-factor and DHpp values suggests that microscopic magnetic interactions increase as particle size increases.

Table 1 also shows that the value of the resonant magnetic field, Hr decreased from 286.5 to 238.4 Oe as the calcination temperature increased. According to the equation:

$g = h\nu / \beta H$

Where h is Planck's constant, v is the microwave frequency, b is the Bohr magneton (9.274x10-21 ergOe-1) and H is resonant magnetic field, the resonance magnetic field, Hr should be decrease when g-factor increases, whereas v is constant in ESR spectroscopy.

CONCLUSION

Spinel nickel manganese oxide ($NiMn_2O_4$) nanocrystals were synthesized by a thermal treatment method using poly (vinyl pyrrolidon) as capping agent to stabilize the particles. As confirmed by XRD, particle sizes ranging from 16 to 51 nm were achieved with calcination temperatures between 400 and 950°C. The FT-IR spectrum confirmed the presence of metal oxides at all temperatures and removed completely at 950°C. Electron spin resonance (ESR) spectroscopy was used to measure three parameter that characterize the magnetic properties, peak-to-peak line width (DHpp), resonant magnetic field (Hr) and g-factor.

ACKNOWLEDGEMENTS

Especially thank to Ministry of Higher Education (MOHE) for financial supports. This work was supported by the MOHE under the ERGS grant.

REFERENCES

[1]. Mehandjiev,D., A. Naydenov, G. Ivanov *Applied Catalysis A: General* **206** (2006) 13–18
[2]. Barth S, Hernandez-Ramirez F, Holmes JD, Romano-Rodriguez A *Prog Mater Sci*, **55** (2010) 563-627
[3]. Goodarz Naseri, M., E.Bin Saion, H.AbbastabarAhangar, M.Hashim, A.H.Shaari *Journal of Magnetism and Magnetic Materials* **323** (2011) 1745–1749
[4]. Peng HY, Wu T *Appl Phys Lett* **95** (2009) 152106-152106
[5]. Bessekhouad Y, Trari M *Int J Hydrogen Energy* **27** (2002) 357-362
[6]. Zhang XD, Wu SZ, Zang J, Li D, Zhang ZD *J Phys Chem Solids* **68** (2007) 1583-1590
[7]. Hosseini, S.A., A. Niaei, D. Salari, S.R. Nabavi *Ceramics International* 38 (2) (2012) 1655-1661
[8]. H W Yan, X J Huang, L Q Chen H W Yan, X J Huang, L Q Chen *Journal of Power Sources* 82, (1-2) (1999) 647-650
[9]. Taniguchi, I., C.K. Lim, D. Song, M. Wakihara *Solid State Ionics* **146** (2002) 239 – 247
[10]. María José Aragón & Pedro Lavela & Bernardo León & Carlos Pérez-Vicente & José Luis Tirado & Candela Vidal-Abarca *J Solid State Electrochem* **14** (2010) 1749–1753
[11]. Fauteux, D. G., A. Massucco, , J. Shi and C. Lampe-O'nnerud *J. Applied Electrochemistry* **27** (5) (1997) 543-549
[12]. Julien, C., E. Haro-Poniatowski, M.A. Camacho-Lopez, L. Escobar-Alarcon, J. Jimenez-Jarquin *Materials Science and Engineering B* **72** (2000) 36–46
[13]. Mahmoud Goodarz Naseri, Elias B. Saion, Mansor Hashim, Abdul Halim Shaari,Hossein Abasstabar Ahangard *Solid State Communications* **151** (2011)

1031–1035.
[14]. Mahmoud Goodarz Naseri, Elias B. Saion, Hossein Abbastabar Ahangar, Mansor Hashim, Abdul Halim Shaari *Powder Technology* **212** (2011) 80–88
[15]. Mahmoud Goodarz Naseri, Elias B. Saion, Hossein Abbastabar Ahangar, Abdul Halim Shaari,1 and Mansor Hashim (2010) Journal of Nanomaterials, Article ID 907686, 8 pages; doi:10.1155/2010/907686
[16]. J.P.Singh, R.C.Srivastava, H.M.Agrawal, R.P.S.Kushwaha *J.HyperfineInteract.* **183** (2009) 393–400
[17]. A. V. Salker, S. M. Gurav *Journal of Materials Science* **35** (2000) 4713-4719
[18]. V.A.M.Brabers *Phys. Status Solidi B* **33** (1969) 563–572
[19]. E.K.Nyutu, W.C.Conner, S.M.Auerbach, C.H.Chen, S.L.Suib *J.Phys.Chem.* **112** (2008) 1407–1414
[20]. S. A. Hosseini, A. Niaei, D. Salari, S.R. Nabavi *Ceramic International* 38 (2011) 1655-1661
[21]. G.Vaidyanathana, S.Sendhilnathan *Physica B* **403** (2008) 2157–2167